



DEPARTMENT OF INFORMATICS

TECHNISCHE UNIVERSITÄT MÜNCHEN

Master's Thesis in Informatics: Games Engineering

Evaluation of rendering optimizations for virtual reality applications in Vulkan

Paul Preißner





DEPARTMENT OF INFORMATICS

TECHNISCHE UNIVERSITÄT MÜNCHEN

Master's Thesis in Informatics: Games Engineering

Evaluation of rendering optimizations for virtual reality applications in Vulkan

Evaluation von Renderoptimierungen für Virtual Reality Anwendungen in Vulkan

Author:	Paul Preißner
Supervisor:	Sven Liedtke
Advisor:	Advisor
Submission Date:	February 15 2020



I confirm that this master's thesis in informatics: games engineering is my own work and I have documented all sources and material used.

Garching bei München, February 15 2020

Paul Preißner

Acknowledgments

Abstract

Virtual reality (VR) and modern low-level graphics APIs, such as Vulkan, are hot topics in the field of high performance real-time graphics. Especially enterprise VR applications show the need for fast and highly optimized rendering of complex industrial scenes with very high object counts. However, solutions often need to be custom-tailored and the use of middleware is not always an option. Optimizing a Vulkan graphics renderer for high performance virtual reality applications is a significant task. This thesis will research and present a number of suitable optimization approaches. The goals are to integrate them into an existing renderer intended for enterprise usage, benchmark the respective performance impact in detail and evaluate those results. This thesis will include all research and development documentation of the project, an explanation of successes and failures during the project and finally an outlook on how the findings may be used further.

Kurzfassung

Contents

Acknowledgments	iii
Abstract	iv
Kurzfassung	v
1 Introduction	1
1.1 Briefly - what's the goal	1
1.2 Industry collaboration	2
1.3 Technical foundation	2
2 The RTG Tachyon Engine	4
2.1 The Engine	4
2.1.1 Render setup	4
2.1.2 Render loop	5
2.1.3 VR render loop	6
3 Stereo Rendering Optimization - Input reduction	8
3.1 Superfrustum Culling	9
3.1.1 Theory	9
3.1.2 Estimated impact	10
3.1.3 Implementation specifics	10
3.2 Round Robin Culling	10
3.3 Conical Frustum Culling	11
4 Stereo Rendering Optimization - Effort reduction	12
4.1 Multiview stereo rendering	12
4.1.1 Theory	12
4.1.2 Estimated impact	14
4.1.3 Implementation specifics	14
4.2 HMD Stencil Mask	15
4.2.1 Theory	15
4.2.2 Estimated impact	15
4.2.3 Implementation specifics	15
4.3 Monoscopic Far-Field Rendering	17
4.3.1 Theory	17
4.3.2 Estimated impact	18

4.3.3	Implementation specifics	19
4.4	MFFR Variant: Depth Shift	20
4.5	MFFR Variant: Alternate eye	20
4.6	Foveated Rendering	21
4.6.1	Theory	21
4.6.2	Estimated impact	21
4.6.3	Implementation specifics	21
5	Performance impact	22
5.1	Explanation - Performance measurements	22
5.1.1	Framerate, frametimes, framepacing	22
5.1.2	Resource usage	22
5.2	Benchmark results	22
5.2.1	Individual impacts	22
5.2.2	Combined and partially combined impacts	22
5.2.3	Interpretation	22
6	Outlook	23
	List of Figures	24
	List of Tables	25

1 Introduction

1.1 Briefly - what's the goal

Real-time rendering is by no means a new research topic. Naturally developers and researchers have devised shortcuts and optimizations in both hardware and software as far back as the first applications in video games, visualization - scientific or otherwise - and simulation. There are methods and algorithms for almost any type of hardware, rendering technique and application scope. One more recently resurged trend is virtual reality (VR). The realization of comparably affordable, comfortable and hassle-free virtual reality headsets like the Oculus Rift series, the HTC Vive, Windows Mixed Reality design or the recently launched Valve Index led to a newfound vigor for the technology among consumers. Similarly, businesses as well as scientists are increasingly looking to VR for various fields of research, marketing opportunities, engineering support and more.

However, virtual reality poses challenges and requirements not commonly seen with traditional real-time applications on monoscopic screens. And while goals such as stable motion tracking and low latency, high performance rendering are as old as early VR HMDs, this recent resurgence has prompted much more active search for possible solutions. Among these requirements is the need for high framerates to give the user a better feeling of visual fluidity and to avoid motion sickness. VR applications need not only render at high framerate, they also need to do so at higher resolutions than common flat screens. As the much lower viewing distance and added lens distortion means pixels appear much larger to the user, the only way to combat visual aliasing and the so called screen door effect is to significantly increase pixel count and density. Similarly to the illustration in [TODO: GPUZEN1 article A], let's assume a traditional console video game running at Full HD resolution and 60 frames per second, a common sight for 8th generation consoles. Meanwhile the same game running in a VR headset may require resolutions and framerate ranging from 1200 pixels per axis per eye at 90 frames per second for entry level headsets up or exceeding 2000 pixels per axis per eye at 120 frames per second for high end devices like the Pimax 4K - not to mention image warp commonly requires and even higher internal rendering resolution by a factor of around 20% or more. In the entry level case that means a resolution increase of roughly 1.6x and a framerate increase of 1.5x for a combined 2.4x power requirement compared to the console baseline, while in the high end case it is roughly 4.6x resolution and 4x framerate uptick for a combined 9.2x power requirement in comparison. [TODO: HMD res illustration?]

While this is very rough napkin math and real applications scale differently to a degree due to a multitude of factors, it paints a clear picture: real-time virtual reality rendering necessitates vastly faster rendering than traditional screens. It obviously follows that VR rendering should take advantage of as much optimization as possible to attain that goal.

There are many established options that are known to improve performance for various if not most application types, with some of these options being de-facto standard features in popular rendering engines. There is also, however, a range of optimizations specific to virtual reality or more generally stereoscopic rendering, and often there is less research and documentation available yet, due in part to aforementioned recent rise in popularity and prior lack of interest.

Thus, this paper aims to collect several of these VR optimizations, implement a subset of them in a real engine and then benchmark and analyse the impact each has on performance. The goal is to have a better collection and understanding of the various methods to use and how much effort may be warranted for each. To this end, what follows is first an explanation of the software and technical foundation used to implement practical samples, then a chapter on optimizations aiming to reduce render *input*, succeeded by a chapter on optimizations aiming to reduce render *effort* and finally an analysis of the performance impact of each implemented approach. Note here that only a subset of the listed methods was implemented due to time constraints.

1.2 Industry collaboration

This thesis is created in collaboration with RTG Echtzeitgraphik GmbH, an engineering and consulting office based in Garching bei München. RTG offers engineering services related to real-time visualization, virtual reality applications and hardware prototyping to enterprise clients from a variety of industry branches such as automotive and industrial logistics. At this point it needs to be disclaimed that the author of this thesis was employed at RTG Echtzeitgraphik GmbH at the time of making. This allowed the use of company assets like workstations, a range of VR headsets and relevant literature as well as expertise with regard to related technologies and enterprise requirements for a rendering engine. The thesis, accompanied research efforts and all material created for the purpose of this thesis, however, are the author's own work.

1.3 Technical foundation

From this industry collaboration follow influences when choosing the technical foundations of the thesis. In an effort to represent a realistic use case, an engine with actual production usage target was chosen as opposed to a purely synthetic "test vehicle", namely RTG's own Tachyon. The engine and its structure is further explained in [TODO: chapter 2 - Tachyon Engine]. The graphics API and library of choice for this thesis then is the Khronos Group's Vulkan. Vulkan is a low level graphics API officially created in 2014 and formally released in early 2016 with the promise of increased flexibility and reduced overhead compared to prior graphics APIs as well as compatibility with a wide range of hardware architectures and operating systems. On the flipside, the verbose and low level nature of the API brings increased development effort and means that these promised improvements can only be

leveraged with sufficient care and caution by developers. More specifically for Tachyon and this thesis, the goal is to enable fast rendering of complex scenes with very large object counts, all while driving virtual reality headsets at high resolution and framerate. To this end, Vulkan promises a good fit. Furthermore Vulkan is seeing a steady growth in developer interest and industry adoption, but with documentation, resources and API-specific research still being lackluster in some ways. This thesis hopes to add useful insights to this pool. Lastly - as a sort of tease to the future - both Vulkan and the VR optimizations presented here are compatible with many ARM-based SoCs running Google's Android as well as Apple's iOS, promising prospects for the category of standalone low power VR headsets which are seeing increasing popularity.

2 The RTG Tachyon Engine

2.1 The Engine

Rendering optimizations can only be implemented if there actually is a renderer at hand. In order to see how the chosen approaches would perform in an engine intended for productive use and industrial applications, rather than an ad hoc renderer only built for some specific tests, Tachyon was chosen, an engine currently in development at RTG Echtzeitgraphik GmbH. Tachyon uses a fully Vulkan based forward renderer (internally called `rtvklib`) with support for multiple viewports of various types, including an OpenVR based virtual reality path, an optional physically-based shader pipeline, a user interface module, a network module and a physics module with more extensions on the development schedule for the future. The renderer integrates Vulkan version 1.1.85 and up and OpenVR version 1.4.18 and up with support for all major SteamVR headsets at the time of writing, including roomscale tracking of the Valve Index, HTC Vive and Vive Pro, the Windows Mixed Reality series and Oculus Rift series.

2.1.1 Render setup

As typical for the verbose nature of Vulkan, render initialization starts with the creation of all necessary basic Vulkan resources such as descriptors, descriptor sets, activation of a minimal set of Vulkan extensions and layers and device enumeration. More specific to `rtvklib`, multiple Vulkan pipelines are active by default:

- a material pipeline offering support for a Phong and a PBR shader as well as geometry and index buffers of arbitrary size
- a skybox pipeline with a simplified skybox shader
- a point cloud pipeline, primarily to allow rendering of LiDAR scan data

To facilitate rendering into multiple viewports, Tachyon uses the concept of render targets. Each render target can reference an arbitrary subset of pipelines, comes with its own set of Vulkan framebuffers, command buffers and render pass and its own virtual camera. Whenever any 3D object is to be loaded, `rtvklib` uses several manager classes to keep track of the various resource types needed for an object. There are managers for geometry, materials, textures and instances among other types. When an object is loaded, the former three hold the respective buffers. When an object is to be rendered, it first needs to be instanced, handled by the latter. An instance references the various geometry and materials of the original object again,

but also holds data specific to individual objects in the virtual world, such as transforms or bounding geometry.

The renderer initialization also encompasses virtual reality through OpenVR. Given a valid OpenVR environment and HMD is detected, a special render target is created with a Vulkan renderpass for multiple views and the respective resources.

2.1.2 Render loop

After all startup and initialization is done, the engine's render loop executes `VKRenderer's Update` and `RenderFrame` functions back to back. These functions are shown in [Listing 3.1] and [Listing 3.2].

```
void VKRenderer::Update()

    mRenderMutex.lock();
    mGeometryManager->Update();
    mMaterialManager->Update();
    mInstanceManager->Update();
    mTextureManager->Update();
    mLightManager->Update();
    mPointCloud->Update();
    UpdateGlobalParamsBuffer();

    for (auto renderTarget : mRenderTargets)
    {
        renderTarget->Update();
        mInstanceManager->FrustumCulling(renderTarget);
    }

    if (mPipelinesInvalid) UpdateRenderPipelines();
    if (mCommandBuffersInvalid) UpdateCommandBuffers();
    mRenderMutex.unlock();
```

Figure 2.1: Renderer update function

`VKRenderer::Update` first prompts all aforementioned managers to update their databases, buffers and anything else they hold in case they are dirty. Then it prompts each render target to update, which may involve camera transformation updates and buffer synchronization for example. Also for each render target, the loop will then have the instance manager perform a frustum culling pass, which will for this target save a conservative list of draw call information for objects visible by this target's camera viewpoints. If any of these updates and culling passes set a pipeline or command buffer state invalid, these will be rebuilt accordingly.

`VKRenderer::RenderFrame` simply prompts each render target to perform its per-frame

```
void VKRenderer::RenderFrame()
{
    if (!mDevice)
        return;

    mRenderMutex.lock();
    for (auto renderTarget : mRenderTargets)
    {
        renderTarget->RenderFrame();
    }
    mRenderMutex.unlock();
}
```

Figure 2.2: Renderer frame render function

rendering operations, be it regular monoscopic output for a traditional viewport or pose tracking and stereoscopic composition for a virtual reality target.

2.1.3 VR render loop

As seen in [TODO: Listing 3.3], the virtual reality render target's `RenderFrame` function is rather straight-forward. As long as the target and compositor are active, it updates the OpenVR device poses and virtual camera transforms. It then renders the stereoscopic views, resolves the multisampling layers into single sample and finally submits both eyes' images to SteamVR, which serves as the chosen OpenVR compatible compositor on Windows systems.

[TODO: overview illustration]

```
void OpenVR::RenderFrame()
{
    if (!mIsActive || !vr::VRCompositor())
    {
        return;
    }

    // update our poses and camera transforms
    UpdateHMDMatrixPose();
    UpdateCameras();

    // render stereo
    [...]
    submitInfo.pCommandBuffers = &mCommandBuffers[mCurrentFrame];
    vkQueueSubmit(queue, 1, &submitInfo, mInFlightFences[mCurrentFrame]);

    // blit/resolve array layers
    [...]
    submitInfo.pCommandBuffers = &mResolveCommandBuffer;
    vkQueueSubmit(queue, 1, &submitInfo, VK_NULL_HANDLE);

    // Submit to SteamVR
    [...]
    for (int i = 0; i < 2; i++)
    {
        vulkanData.m_nImage = (uint64_t)mResolveImage[i];
        vr::VRCompositor()->Submit(static_cast<vr::EVREye>(i),
            &texture, &bounds);
    }
}
```

Figure 2.3: Renderer frame render function

3 Stereo Rendering Optimization - Input reduction

When looking at real-time rendering as it is done today - albeit from a strongly simplified perspective - the CPU could be described as a employer and the GPU as an employee. For each frame, the CPU produces certain render tasks and supplies the necessary information such as draw calls, shader parameters, buffers and so forth. The GPU then consumes these tasks and associated items and dos the heavy lifting to produce the required results. Now if one wants to speed up that overall process, there are two major ways. One way is to reduce the amount of data that is put into the pipeline so less data needs to be processed overall, the other way is to increase the efficiency of the processing itself. This first chapter of optimization approaches presents ways of reducing the amount of data or work input.

(Hierarchical) Frustum culling

The following options build on top of the regular frustum culling concept. In this the objects in the scene are checked against a camera frustum whether they are inside or outside of it or intersecting with the surface of the frustum. The checks themselves can be generally optimized in various ways, regardless of whether stereoscopy is desired or not. Often only an object's bounding geometry is checked, collections of objects can be precomputed so larger numbers may be discarded at once. An advanced option of culling is to delegate the calculations into a GPU compute shader so potentially less data needs to be transferred from the CPU per frame and much higher vector/matrix calculation is gained in exchange for slower branching. Some modern renderers also do very granular culling like bitmasked checks of precomputed triangle sets, as seen in Ubisoft's Anvil Next engine used in Assassin's Creed Origins [TODO: Source]. Another optional layer of the culling process is to maintain hierarchical container structures for the scene objects so larger numbers can be discarded or included early on. For all those options the goal is the same, to get as result the list or buffer of objects visible by the given camera frustum in the scene.

Frustum culling in Tachyon

The frustum culling approach in Tachyon is fully CPU-based and utilizes pre-computed hierarchical draw buffers. More specifically, at startup the scene is divided into a coarse grid of [chunks](#) where each grid possesses an octree. Also at startup, a thread pool with the current number of hardware threads is created. At asset load time, these octrees are populated with the loaded objects through optimistic size-aware insertion. Each cell of a tree

then precomputes a draw buffer containing a combined draw call for all objects associated with that cell. These buffers can be recomputed at any time, but the operation should be avoided at runtime as it incurs costly CPU to GPU transfers. In a culling pass, first all `chunks` within a certain draw distance radius of the camera are chosen, so there is an additional very primitive distance culling taking place. Then each `chunk` submits a culling call using its tree to the thread pool. Each such call works as follows:

[TODO: blablabla, Figure etc]

3.1 Superfrustum Culling

3.1.1 Theory

The basic idea behind Superfrustum culling is to essentially do regular frustum culling despite rendering into two cameras, one per eye. The naive way of extending the frustum concept to a stereoscopic camera is to add a second frustum so there is one per eye, then perform the culling check for both frusta and merge the results. As is easily visible from [TODO: Figure X.x] though, the spatial proximity of these two frusta leads to a large overlap volume, especially as field of view increases with more advanced headsets. One possible strategy to leverage more performance when culling two eyes is a so-called Superfrustum, assuming the frustum is the common six sided trapezoid. Cass Everitt of [TODO: Facebook LLC], formerly [Oculus LLC] has suggested this approach at [TODO: Oculus Connect 5?] and provided computation sketches at [TODO: FB source]. The idea is to combine the left and right eye frusta by taking the respective widest outer FOV tangent - usually the left eye's right side and the right eye's left side - and using these as the new side tangents of the superfrustum. Another way to express these is to take the widest half opening angles of each eye and adding them up to a combined opening angle. Similar is done for the top and bottom tangents, although these will usually be nearly identical for the two eyes. A pitfall of the superfrustum is its necessary depth recession. This is easy to visualize when combining the two frusta by extending aforementioned side tangents backwards until they cross. The meeting point of this step is the new origin of the superfrustum, slightly recessed behind the two separate eyes. [Name Surname?] of Silicon Studios offered a generalized way to compute this recession for un-mirrored eye orientation, while Everitt has extended his sketches by an asymmetry normalization. Both of these are important to consider as virtual reality headsets can have slightly canted and asymmetrical lenses, either by design or by manufacturing tolerance. Ignoring these two corrections may still result in a sufficient superfrustum if computed conservatively, but should be included for fully correct setups. While this superfrustum naturally eliminates all overlap of the naive variant, it in turn includes small false positive regions, notably the triangular void found close to the origin points between the two eye frusta and potential side edge regions in the case of asymmetrical lens orientations. In a typical application, the performance cost of these will be negligible.

[TODO: Figures/illustrations by Everitt and Silicon]

3.1.2 Estimated impact

The impact of using a Superfrustum will depend very specifically on the type of frustum culling done and combination with other techniques. On its own with a CPU based culling pass only an appreciable benefit in CPU rendering time is to be expected as the number of frustum checks will be reduced by up to 50% and only a single buffer needs to be transferred to the graphics unit. The GPU itself still needs to render each eye separately though, including all vertex transformations, pixel shading and so forth. The specific impact in the case of Tachyon is elaborated on in [chapter 5]. Superfrustum culling when performed directly on the GPU obviously has great potential to significantly cut down on related compute work, once again to the effect of up to 50% versus a baseline dual frustum culling. An interesting point to consider is whether any of the culling data needs to be synchronized back to the CPU, as when not, the GPU compute workload will only depend on a single small buffer or pushconstant transfer containing the camera parameters. If, however the resulting culling set is transferred back to the CPU, for example for preprocessing of the next frame, this transfer will of course present another speedup limiter.

3.1.3 Implementation specifics

To facilitate Superfrustum culling in Tachyon required only straight-forward changes. At creation time of the virtual camera, the superfrustum is computed from the given OpenVR eye parameters following Everitt and Silicon's way. [TODO: pseudo code?] The calculated superfrustum recession and new combined field of view angles are saved and used every frame when re-transforming the superfrustum. The frustum transformation uses a simple geometric approach where the camera's world position, forward and up vectors in conjunction with the near and far distance, field of view and aspect ratio are extruded into the six planes of the frustum volume. The per-frame culling pass of Tachyon then naturally only checks against this single frustum and returns a single set of draw commands that are then sent to both eyes.

3.2 Round Robin Culling

Another culling variant specific to stereoscopy uses the round robin principle. The concept again springs from the desire to avoid frusta overlap, but instead of combining the frusta, it exploits a common property of current stereoscopy rendering techniques. As modern headsets use circular lens optics and flat displays distorting the displayed image, the framebuffer commonly need to be warped [distorted?] to compensate so the picture looks undistorted to the user again. As a result a lot of the edge data of the image is either considerably squeezed together or outside of the visible area of the HMD displays. This conservative property means a virtual eye frustum can be smaller than the technical frustum of that respective eye and false negative discards in these edge regions would go unseen by the user. Assuming both eyes of the headset have similar opening angles and parallel or nearly parallel viewing direction, the overlap of the two frusta would in most cases encompass the entire stereo-visible volume. So

it naturally follows that only culling for one of the eye frusta would already give a sufficient representation of the actually visible scene.

However, there is still a possibility of missing a few edge cases with this alone. So the extension of the idea to actual round robin assumes another common property of modern VR headsets, namely high refresh rates. Many of these aim for at least 80Hz (Rift S, WMR) ranging up to 144Hz (Index experimental mode) image refresh to give the user a smooth visual sensation. Exactly halving that refresh rate and reprojecting images for two refresh cycles with some pixel interpolation is an established way to still provide an acceptable experience with minor visual artifacting on slower devices as demonstrated by [TODO: Oculus LLC]’s Asynchronous Space Warp [TODO: and/or Time Warp?] and SteamVR’s reprojection features. It follows that a conceivable compromise is to alternate which frustum is used for culling in a round robin fashion so that even if edge cases include visible false negatives, they only persist for one frame at a time. In the worst case this would manifest as shimmering or flickering at the outer edges of the visible screen area.

Overall this makes Round Robin Culling a viable candidate on systems with very limited culling performance, but the tight constraints for sufficiently accurate results make it unfit as a general recommendation.

[TODO: small illustration]

3.3 Conical Frustum Culling

This third alternative culling extension targets the circular shape of HMD lenses for leverage. Coming back to the conservative framebuffer size from the previous section, the lenses lead to a lot of invisible area in the corners of the display. [TODO: Student BA dude] attempts to demonstrate the method in [TODO: BA paper] albeit with limited success. That proof of concept does show the validity of the method though. The traditional six sided trapezoid frustum is replaced by a cone encompasses a volumetric projection of the view through each respective lens. For a more geometry-bound GPU, this method will provide a small relief.

[TODO: more specific calculation approach from paper] [TODO: small illustration]

Merging approaches

A convenient side effect of these three presented optimizations is that they can in part be merged. It is conceivable, for example, to do Conical Round Robin Frustum Culling in an effort to slice away as much of the conservative invisible area as possible and reduce the list of drawable objects to an optimistic minimum. It is also possible to construct a Conical Superfrustum aiming to avoid the mentioned edge false positives, albeit only feasible if the display per eye is square-like to avoid adding new false positive volume on other sides.

4 Stereo Rendering Optimization - Effort reduction

This second chapter of optimization approaches targets the efficiency of rendering processes on the graphics chip itself. These approaches have little to no impact on CPU performance and tend to exploit and scale mostly with GPU power.

4.1 Multiview stereo rendering

4.1.1 Theory

When rendering a stereo image using the naive method of simply going through the entire rendering pipeline once for each viewport, potentially a lot of computation is done twice with little or no change in data or parameters. With the [TODO: general graphics pipeline, Figure x.x] in mind, it's clear that for example the vertex stage will see very little change in output as geometry and index buffers are largely the same between multiple stereo viewport passes with only minor shifts in the view matrices. Similarly, the geometry stage is commonly not dependent on specific eye data and as such would be a waste to process with the same data twice [TODO: check again]. Once the rasterizer stage of the pipeline is reached, the situation changes as stereo separation means the two images have notably different content and work from one can not realistically be recycled in the other.

An optimization exploiting this is called multiview stereo rendering, and very quickly surfaced as an idea after the introduction of the Nvidia Geforce 8 and ATi Radeon HD 2000 series in 2006 brought unified shader architectures to the market [TODO: source]. Prior architectures relied on separate vertex and pixel shader units with relatively fixed capabilities and few ways to share data. Fully programmable shader units then allowed more customizable and efficient pipeline usage necessary for multiview to show any benefit. The lack of mainstream stereoscopic systems prohibited the feature from becoming more important until the official introduction of multiview extensions to graphics APIs like OpenGL ([GL_OVR_multiview](#)) and Vulkan ([VK_KHR_Multiview](#), previously [_KHX](#) and [_NV](#)). The same resurgence saw the idea expanded and further optimized and - in more recent vendor specific terms - Nvidia calling it Single Pass Stereo, Simultaneous Multi-Projection and Multi-View rendering and AMD calling it LiquidVR multiview. The idea behind all these terms is the same, albeit with detail differences between the different flavors.

The core concept of multiview rendering is to submit all draw commands for a stereoscopic

frame in one call instead of two separate passes, which can cut down CPU render and transfer time depending on the type and amount of data pushed to the GPU. Expensive synchronization barriers are essentially halved and all necessary writes are performed in a single go. As an addition, *hardware* multiview rendering is to only perform those pipeline stages multiple times that actually produce notably different data for each eye, such as the rasterizer and pixel shader stages, while only running the earlier stages with little changes once. The data from stages run only once can then be reused by the multiply run stages with very little extra cost. This expanded technique improves pipeline efficiency and will scale heavily depending on workload. For fragment-heavy applications the benefit will be limited while high vertex or geometry loads tend to scale more optimally. Hardware acceleration requires additional registers and pipeline shortcuts in the chip itself though, which constraints it to more modern GPU architectures built with it in mind [TODO: Source Nv GDC 2015, etc]. Nvidia could be considered the main progress drivers for this, having pushed the technology from parallel geometry projection in Maxwell's Multi-Projection Acceleration to Pascal's SMP which adds lens-matched shading to better approximate the lens shape and finally to Turing's Multi-View with a doubling of available views and positional independence to support state of the art HMDs with canted displays [TODO: nvidia sources].

[TODO: illustration]

The small tradeoff then is that all relevant view data for each viewport has to be handed to the pipeline at once, creating a little higher memory overhead. Additionally certain buffers such as geometry and indices for the vertex stage need to be uniform across all viewports and can't be altered for each eye as they are processed in a single pass. [TODO: is there any warping happening? -> very slight artifacts possible]

Going by the user-maintained Vulkan Hardware Database [<https://vulkan.gpuinfo.org/listreports.php?exte>]
The major GPU vendors specify multiview support in their architectures as follows:

- Nvidia: hardware multiview from the Maxwell generation and newer, software support from Kepler onward
- AMD: software support from Graphics Core Next 1.0 onward [TODO: hw support?]
- Intel: software support begins with Generation 9.0 (Skylake/Apollo Lake GT) onward under Windows, Generation 7.0 (Ivy Bridge GT) onward under Linux [TODO: hw support?]
- Qualcomm: software support from Adreno 500 onward
- ARM: software support from Bifrost onward, limited support on Midgard
- Imagination: software support from Rogue onward

Note here while support of the desktop parts is solid and stable, the ARM-based mobile chipsets often have incomplete or unstable drivers [TODO: source]. For all submitted devices (892 at the time of writing) the database shows support coverage of 54% on Windows systems,

69% on Linux systems and only 23% on Android. This statistic may not be very reliable, however, as an undetermined portion of the submissions contains incomplete or flawed information such as drivers versioned as 0.0.0 or API versions reported as 0.0.1.

4.1.2 Estimated impact

Impact of this extension is highly dependent on the specific workload, the used graphics hardware and renderer structure. [TODO: AMD LiquidVR numbers, Anand SMP tests, Nv MV dev blog]

4.1.3 Implementation specifics

In Vulkan specifically, multiview is enabled through the [VK_KHR_multiview](#) extension. This extension's availability on the target hardware can be queried and if available, the individual hardware-dependent implementation is abstracted by Vulkan.

In the Tachyon implementation of multiview, the following changes to the render loop are introduced:

- The VR render target adds [VK_KHR_GET_PHYSICAL_DEVICE_PROPERTIES_2](#) to the required instance extensions and [VK_KHR_MULTIVIEW](#) to the required device extensions during Vulkan instance and device creation at startup
- the previously separate per-eye VR render passes are merged into a single render pass
- this VR render pass incorporates the multiview pNext extension using a view mask and correlation mask of 0x11, with each of those bits representing one of the eyes
- the Frustum Culling pass combines the two frustum checks with an early accept and outputs a merged set of draw call information
- the second command buffer recording - previously intended for the second eye - in [OpenVR::RecordCommandBuffers](#) is cut out as multiview render passes can only take a single unified set of command buffers
- the underlying GLSL shader is modified to pick camera parameters based not only on a given camera index, but also the implicit [gl_viewIndex](#) as Vulkan multiview uses this integer to index the current viewport

The VR render target's framebuffer, color attachment and depth attachment are already set up as dual-layered buffers which makes them readily compatible with multiview render passes. With these changes, the Tachyon renderer is fully switched over to single pass stereo rendering.

4.2 HMD Stencil Mask

4.2.1 Theory

Introduced to the mass market with 3Dlabs' Permedia II in 1997 and widely adopted since then, all modern graphics chips support a nifty feature called the stencil buffer. This buffer uses low bit integer values - commonly 8 bits per pixel for a depth of 256 [TODO: <https://learnopengl.com/Advanced-OpenGL/Stencil-testing>] that can be read from and written to during the fragment stage, with stencil testing happening after alpha and before depth testing. Sometimes used for certain shadowing operations, the stencil buffer is primarily used for cheap masking efforts.

One such effort was presented by [TODO: Valve dude] at [TODO: GDC 2015] as a possibility to improve performance in VR applications. Once again pointing at the significant areas of invisible screen space wasted outside the HMD lenses' warping reach, the idea here is to write into a per-eye pixel matched stencil buffer a mask corresponding to the shape of the visible screen area. Then during the fragment stage of a frame render, the stencil test can early discard all masked fragments and thus avoid pixel shader work for all these areas. The operation can essentially be imagined exactly as the classic idea of stencil mask when painting surfaces, where paint will only hit the surface within the cutouts of the stencil. Similarly the graphics chip will only write color and depth values to unmasked fragments. [TODO: illustration]

4.2.2 Estimated impact

The performance gain then naturally scales well with both increased fragment shader bias of the per-frame workload as well as with the HMD's blind areas. Valve's [TODO: dude] in his GDC talk showcased gains of 17% lower GPU frametimes for the company's Aperture Labs VR showcase scene using an HTC Vive headset. [TODO: verify] Assuming a roughly uniform distribution of objects in the scene and accordingly a roughly constant shader workload during use, the relative improvement in fragment render time is directly proportional to the masked percentage of the total framebuffer. [TODO]

4.2.3 Implementation specifics

Outfitting Tachyon for stencil masking required the addition of the entire stencil stack as the engine did not use the feature in any capacity yet. An inherent advantage of this is that it allows to render the stencil mask only once at startup and keep reusing it every frame without additional render load for the mask.

The changes include extending the depth attachment of the OpenVR render pass with the `VK_IMAGE_ASPECT_STENCIL_BIT` so the additional buffer layer is created at startup. What's more, the involved Vulkan pipelines need stencil operation states defined in their `VkPipelineDepthStencilState` with the operations set as in [TODO: Figure] so the bits are checked against but not modified. Next, the VR render pass needs its color attachment's `stencilLoadOp` set to `VK_ATTACHMENT_LOAD_OP_LOAD` so the renderer knows to load the stencil buffer at the start

of the color pass, and the `stencilStoreOp` to `VK_ATTACHMENT_STORE_OP_DONT_CARE` so it can leave the buffer behind after use without saving anything more to it. This is important to make sure our stencil buffer remains unmodified and expensive writes are avoided.

```
//stencil op settings for pipelines using the stencil mask for comparison
VkStencilOpState stencilOpState = {};
stencilOpState.compareOp = VK_COMPARE_OP_NOT_EQUAL;
stencilOpState.failOp = VK_STENCIL_OP_KEEP;
stencilOpState.depthFailOp = VK_STENCIL_OP_KEEP;
stencilOpState.passOp = VK_STENCIL_OP_KEEP;
stencilOpState.compareMask = 0xff;
stencilOpState.writeMask = 0xff;
    [TODO: check what both masks do]
stencilOpState.reference = 1;
```

Figure 4.1: Stencil operation bits set for default material Pipeline

Rendering the stencil mask itself at startup is done as follows: OpenVR by now has some helper functions for masking built in, such as the `GetHiddenAreaMesh(EVREye eEye)` function that returns as screenspace normalized list of vertices representing the ideal mask mesh for the current HMD as known to OpenVR. [TODO: check "ideal"ity for various HMDs] The obvious benefit of this is the simplicity of getting a fitted mask for most HMDs instead of either approximating with circular masks or going through the trouble of manually creating fitted meshes for existing and coming OpenVR-enabled headsets. Unfortunately, however, OpenVR in a few instances returns empty masks, such as for the Oculus Rift CV1. For those cases a fast circular approximation mask may be an adequate compromise.

Tachyon queries OpenVR for the mesh of each eye, converts the vertex lists into a renderer-compatible vertex format and writes out a vertex and index buffer each. At the end of the VR render pass, an ad-hoc command buffer is recorded and submitted to render the two masks into the VR framebuffer's depth attachment's stencil layer. The `VK_IMAGE_ASPECT_STENCIL_BIT` is set to ensure only that layer is written to.

Due to Vulkan's verbose nature, rendering these two masks also requires its own pipeline. The default material pipeline, PBR pipeline et cetera only do stencil test compares, no writes, they perform color writes and rasterizer face culling, all things the stencil mask pipeline should do differently. So a separate stencil pipeline is introduced with stencil operation state set like in [TODO: Figure], color writes masked off and rasterizer culling disabled. Should the need to perform per-frame stencil writes arise, merging the material pipelines and the stencil pipeline may prove beneficial to avoid expensive pipeline re-binds, but for the sake of cleaner separation the described setup was used in Tachyon's current implementation.


```
//stencil op settings for the stencil pipeline
VkStencilOpState stencilOpState = {};
stencilOpState.compareOp = VK_COMPARE_OP_ALWAYS;
stencilOpState.failOp = VK_STENCIL_OP_REPLACE;
stencilOpState.depthFailOp = VK_STENCIL_OP_REPLACE;
stencilOpState.passOp = VK_STENCIL_OP_REPLACE;
stencilOpState.compareMask = 0xff;
stencilOpState.writeMask = 0xff;
[TODO: check what both masks do]
stencilOpState.reference = 1;
```

Figure 4.2: Stencil operation bits set for stencil mask Pipeline

4.3 Monoscopic Far-Field Rendering

4.3.1 Theory

Monoscopic Far-Field Rendering (MFFR) is a curious approach strongly aligning with an inherent property of many optimizations in the field of rendering and real-time computing in general, which is the property of trading accuracy for speed. MFFR is a topic brought up again in the early days of Rift CV1's retail launch by [TODO: Oculus? Epic? check timeframe] at developer keynotes.

Understanding the concept requires some explanation of the technical and visual background. Proper depth perception of the human eye relies on the slight spatial distance between both eyes as each eye sees a slightly different angle of a given object. This difference in perceived angle is called stereo separation [TODO: word this more scientifically?] and without it, the brain has a hard time determining the depth of and at which a certain object or surface lies. Regular stereo rendering obviously recreates this separation correctly when rendering the two virtual eyes at their respective spatial offset from the HMD center - given correct projection and view matrices and accurate world scale at least. However, and that's one aspect MFFR exploits, as distance grows, stereo separation shrinks. In infinity, separation would be infinitely small, but even at more reasonable distances separation becomes so small that even with good vision it becomes hard to properly judge depth unless the object is large. This of course also holds true for rendered stereoscopy, but an additional limit is the pixel density of the output displays. What this means is that at a certain distance from the virtual camera, stereo separation will shrink to less than a full screen space pixel once projected. Obviously if the difference can physically not be displayed by the HMD, it seems a waste of resources to still render both eyes.

Mono Far-Field Rendering thus opts to skip the second view during rendering of the name-giving far field of objects. The hope here is that only rendering a single view past a certain distance reduces rendering load without the user noticing the theoretical loss in accuracy. This approach has caveats unfortunately. For one, the value at which a field split - the distance at which the stereo rendering is cut off and followed by only mono rendering - will depend

on the individual user, their quality of vision and spatial recognition [TODO: better word for that]. It will also potentially depend on the resolution of the used headset given the user's vision is good enough to not deteriorate before that point.

Note here, this thesis will not explore these constraints of MFFR further than approximate values used for testing as time does not allow more.

MFFR has been implemented by Oculus LLC and Epic Games Inc in Unreal Engine 4 at some point and was recommended for example for certain types of mobile VR experiences with very limited GPU power, but curiously has been removed from the engine in update 4.20 without further explanation. An odd decision surely, as Oculus LLC developer blog posts prior to the removal indicated continued optimization efforts such as added compatibility with UE4's multiview path.

[TODO: illustration]

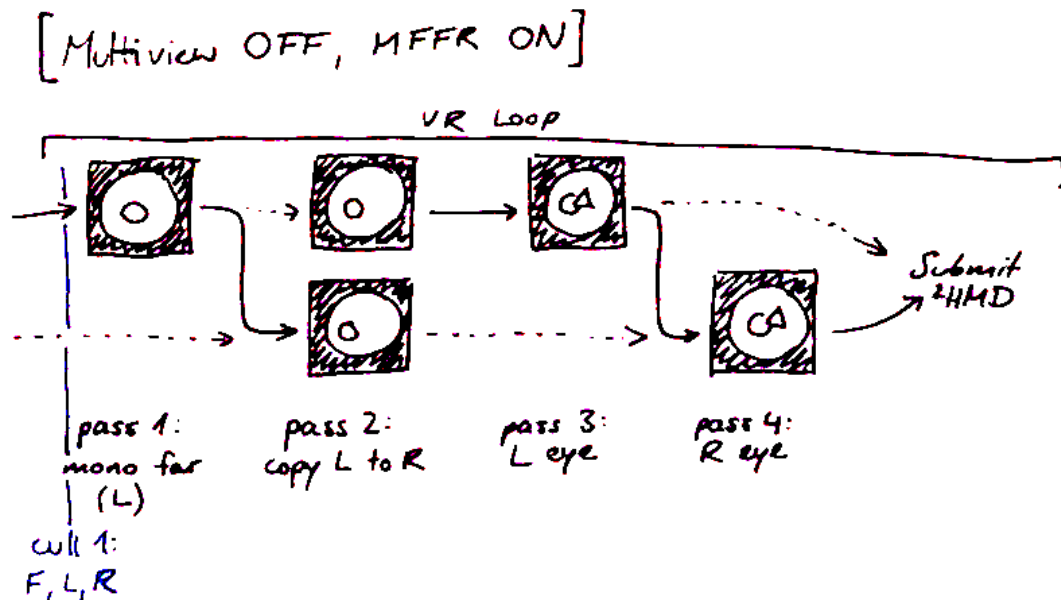


Figure 4.3: [TODO: Monoscopic Far-Field rendering flowchart]

4.3.2 Estimated impact

The makeup of the scene itself will also affect effectiveness of the solution. As cautioned by Oculus LLC in their developer reference on Mono Far-Field Rendering [TODO: src], there is a certain baseline overhead simply for enabling the additional render pass necessary for the monoscopic image and the associated context switches. Furthermore only scenes with a significant of distant geometry beyond the field split distance will benefit from the optimization, as obviously the second view workload can only be saved for objects that would be contained within that second pass. [TODO]

4.3.3 Implementation specifics

Implementing Mono Far-Field Rendering into Tachyon - or any renderer for that matter - requires care and a number of changes. In this case, the plan was to do MFFR as illustrated in Figure 4.3, by way of two render passes but only a single framebuffer. In the first step of each VR frame, a monoscopic render pass would render the far clip volume into the index 0 layer of the framebuffer [TODO: ...can Vulkan be set to write pixels into two buffers at the same time?]. The next step would copy that layer to index 1 as well. In the final step then the regular stereoscopic render commands would be executed with reduced near field clip volume. The goal of this approach is to reduce memory operations and locality to a minimum and also avoid more costly compositing methods. While the general approach sounds straight-forward, implementing it in a Vulkan renderer is no trivial task and required the following changes to the renderer:

- for the virtual camera, a field split distance parameter is introduced and an additional frustum is added - the stereo frusta then cover the volume from near plane to split plane while the far field frustum covers split plane to far plane
- the frustum culling procedure is altered to write the far frustum's resulting draw commands into a separate set instead of merging them into one (as would happen for regular multifrustum culling in Tachyon)
- at initialization time of the VR render target, an additional render pass is created for monoscopy, with the main difference compared to the VR render pass being that it foregoes the multiview extension
- add an additional set of Vulkan `VkCommandBuffers` into which the draw commands of the far frustum cull set are to be recorded
- add an additional set of `VkSemaphores` to synchronize the two render passes and create them in `CreateSyncObjects()` during initialization
- add an additional `VkCommandBuffer` for the layer copy operation
- at initialization time of the VR render target, pre-record this copy command buffer so it can be reused every frame; this recording includes transitioning the layout of both the color and depth image from `VK_IMAGE_LAYOUT_TRANSFER_SRC_OPTIMAL` to `VK_IMAGE_LAYOUT_GENERAL`, `vkCmdCopyImage(...)` both images' layer 0 to layer 1 and then transition the layouts in reverse again
- in the per-frame recording procedure of the VR render target, `RecordCommandBuffers(...)`, the entire structure of begin and end of command buffers and render pass and per-pipeline `RecordDrawCommand(...)` calls is duplicated with the monoscopy render pass and far field command buffers set; after that block the prior regular stereo recording still takes place

- in the render target's `RenderFrame(...)` function the far field command buffer and layer copy command buffer submission is inserted before the regular stereo submits; the mono submit is set to wait on `mRenderCompleteSemaphores` and signal `mFarfieldCompleteSemaphores`, the latter of which the stereo submit is set to wait on
- in VR render target's camera setup, construct the far field frustum projection matrix as outlined in [TODO: Vulkan Cookbook?] - transposed as Tachyon still retains OpenGL matrix format for a few matrix types
- add an additional set of camera data struct and camera index
- in the render target's `UpdateCameras()` call, update the far field volume's view projection matrix by transforming aforementioned projection matrix by the current HMD pose and write that updated matrix to the camera data buffer on the GPU

[TODO: sort this list a bit better? normal text some of it?]

Some issues with this implementation do prevail and make it unfit for productive deployment, unfortunately. For one, while the lack of pure separation at little to not sideways tilt is acceptable and not easily noticed, tilting the head means more severe separation mismatch as the spatial disconnect is expanded from being mostly horizontal to being horizontal and vertical. [TODO: check whether it works any better with different proj matrices (e.g. more akin to L eye?)] [TODO: example picture comparison]

4.4 MFFR Variant: Depth Shift

MFFR in its basic version as described above obviously completely foregoes separation beyond the split distance and as such that split distance has to be set relatively far back to minimize the visual inaccuracy. So naturally it seems profitable to attempt to try and reduce that split distance closer to the camera by artificially increasing that accuracy again. One such way is to use the data already contained in the framebuffer's depth layer during rendering. As stereo separation is mostly dependent on depth given the object itself and its properties are known, it is logical to approximate small amounts of separation based on that depth buffer. Instead of simply copying layer 0 to layer 1 after the far field pass, one can do a sampling pass over layer 1 from layer 0 or a post-processing pass after the copy operation and slightly shift pixels according to the depth value of the respective given fragment. [TODO: some math? illustration]

4.5 MFFR Variant: Alternate eye

[TODO]

4.6 Foveated Rendering

4.6.1 Theory

[TODO]

4.6.2 Estimated impact

[TODO]

4.6.3 Implementation specifics

[TODO]

5 Performance impact

5.1 Explanation - Performance measurements

5.1.1 Framerate, frametimes, framepacing

5.1.2 Resource usage

5.2 Benchmark results

5.2.1 Individual impacts

5.2.2 Combined and partially combined impacts

5.2.3 Interpretation

6 Outlook

[TODO]

List of Figures

2.1	VKRenderer's Update	5
2.2	VKRenderer's RenderFrame	6
2.3	OpenVR render target's RenderFrame	7
4.1	Material pipeline stencil operation bits	16
4.2	Stencil pipeline stencil operation bits	17
4.3	[TODO: Monoscopic Far-Field rendering flowchart]	18

List of Tables